OPEN ACCESS

University of BRISTOL

Peer reviewed version

Link to published version (if available):
10.1063/1.5085281

Link to publication record in Explore Bristol Research
PDF-document

University of Bristol - Explore Bristol Research
General rights

A chalcogen-bonded complex $H_3N\cdots S=C=S$ formed by ammonia and carbon disulfide characterised by chirped-pulse, broadband microwave spectroscopy

Eva Gougoula, [a] Chris Medcraft,[b] Ibon Alkorta,[c] Nicholas R. Walker,[a*] Anthony C. Legon [d*]

[a] *Chemistry-School of Natural and Environmental Sciences, Newcastle University, Bedson Building, Newcastle-upon-Tyne NE1 7RU, UK*

[b] *School of Chemistry, University of New South Wales, New South Wales 2052, Australia*

[c] *Instituto de Química Médica (IQM-CSIC), Juan de la Cierva, 3, E-28006 Madrid, Spain*

[d] *School of Chemistry, University of Bristol, Cantock's Close, Bristol BS8 1TS, UK*

Abstract

Ground-state rotational spectra were observed for ten symmetric-top isotopologues $H_3N\cdots S=C=S$, $H_3N\cdots^{34}S=C=S$, $H_3N\cdots S=C=^{34}S$, $H_3N\cdots S=^{13}C=S$, $H_3^{15}N\cdots S=C=S$, $H_3^{15}N\cdots^{34}S=C=S$, $H_3^{15}N\cdots S=C=^{34}S$, $H_3^{15}N\cdots S=^{13}C=S$, $H_3^{15}N\cdots^{33}S=C=S$ and $H_3^{15}N\cdots S=C=^{33}S$, the first five in their natural abundance in a mixture of ammonia and carbon disulphide in argon and the second group with enriched $^{15}NH_3$. The four asymmetric-rotor isotopomers $H_2DN\cdots S=C=S$, $H_2DN\cdots^{34}S=C=S$, $H_2DN\cdots S=C=^{34}S$, and $HD_2N\cdots S=C=S$ were investigated by using a sample composed of ND_3 mixed with CS_2. Rotational constants, centrifugal distortion constants and ^{33}S nuclear quadrupole coupling constants were determined from spectral analyses and were interpreted with the aid of models of the complex to determine its symmetry, geometry, one measure of the strength of the intermolecular binding, and information about the subunit dynamics. The complex has C_{3v} symmetry, with nuclei in the order $H_3N\cdots S=C=S$, thereby establishing that the non-covalent interaction is a chalcogen bond involving the non-bonding electron pair of ammonia as the nucleophile and the axial region near one of the S atoms as the electrophile. The small intermolecular stretching force constant $k_\sigma = 3.97(5)$ N m^{-1} indicates a weak interaction and suggests the assumption of unperturbed component geometries on complex formation. A simple model used to account for the contribution of the subunit angular oscillations to the zero-point motion leads to the intermolecular bond length $r(N\cdots S) = 3.388(10)$ Å.

* Corresponding authors: a.c.legon@bristol.ac.uk; nick.walker@newcastle.ac.uk

1. Introduction

A wide range of non-covalent, pairwise interactions of molecules in the gas phase has been investigated spectroscopically in the last 50 years. The most important of these is the hydrogen bond because of its ubiquity in Chemistry and Biology. The halogen bond has become of increasing interest since the 1990's and its properties have been shown[1,2] to parallel those of the hydrogen bond in many respects. Modern definitions[3,4] of both these important interactions have been published recently. Tetrel, pnictogen, chalcogen and coinage-metal bonds are less well known non-covalent interactions and were given names only during the last seven years,[5-8] even though they had been characterised extensively in the gas phase during the last 50 years.[9]   These newer types of pairwise interaction can be
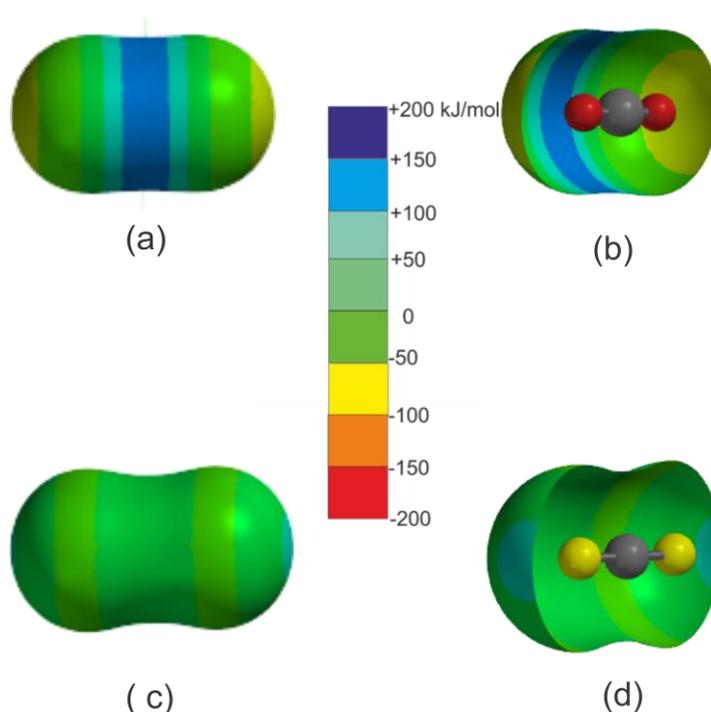
Figure 1.   Molecular electrostatic surface potentials (MESPs) on the 0.002 e/bohr^3 of carbon dioxide (a) and (b) and carbon disulphide (c) and (d) calculated at the MP2/6-311++G** level using SPARTAN.   In (b) and (d), each surface has been rotated by several degrees about the C_2 axis and the front half removed.

written in general as B···E–R, where E is an atom of group 14, 15, 16 or 11, respectively, R is the remainder of the molecule E–R, and B is a Lewis base. The atom E is the most electrophilic region of E–R and interacts with a nucleophilic region of B, usually a non-bonding (n) electron pair or a π-bonding electron pair. As an example, the C atom is the most electrophilic region of CO_2 and interacts with the n-pair of NH_3 to form a T-shaped complex in which the linear CO_2 molecule acts as the bridge of the T while the C_3 symmetry axis of NH_3 forms the stem.[10] Thus, the weak intermolecular bond is a tetrel bond.

Carbon disulphide CS_2 is an isostructural congener of CO_2 and therefore might be expected also to form tetrel bonds in which its C atom again acts as the electrophilic region when interacting with Lewis bases such as NH_3. Examination of the molecular electrostatic surface potentials (MESP) of CO_2 and CS_2 calculated at the MP2/6-311++G** level with Spartan[11] and shown in Figure 1 reveals that the electrophilic (blue, most positive potential) region is differently placed in these two molecules, however. CO_2 has an electrophilic (blue) band around the C atom while CS_2 has no such band, but instead its most electrophilic region lies near each S atom along the C_∞ axis. This indicates that CS_2 and NH_3 are likely to form a complex $H_3N···S=C=S$ of C_{3v} symmetry. To the best of our knowledge, the only complex of CS_2 investigated by means of its rotational spectrum is that with H_2O, for which Ogata and Lovas[12] report that the most probable geometry is $H_2O···S=C=S$, planar with C_{2v} symmetry.

We report here a detailed investigation, by chirped-pulse broadband microwave spectroscopy, of the ground-state rotational spectra of fourteen isotopologues of a complex formed by ammonia with carbon disulphide. Interpretation of the spectroscopic constants thereby determined in the light of a simple model of the complex allows the symmetry, the order of the atoms, the geometry, the strength of binding (as measured by the intermolecular stretching force constant k_σ) and information about the subunit dynamics to be derived. The

results can then be compared with those from good quality *ab initio* calculations, as recently published.[13]

2.   Experimental

The chirped-pulse, Fourier-transform microwave (CP-FTMW) spectrometer used at Newcastle University has been described in detail elsewhere.[14] The spectrometer can be configured to operate in either the 2.0-8.0 or 7.0-18.5 GHz frequency bands during individual experiments. Spectra were recorded across each of these bands during the present work.

The generation of $CS_2 \cdots NH_3$ was achieved by mixing CS_2 and NH_3 within an argon buffer gas and pulsing this sample through a supersonic valve (Parker, General Series 9) into a vacuum chamber at a backing pressure of 7 bar. Each of CS_2 and NH_3 were present in the gas sample at low concentrations of 1% and 2% respectively. Isotopically-enriched samples of $^{15}NH_3$ or ND_3 were used to permit experiments on isotopologues containing ^{15}N or D respectively. Coherent polarisation of the molecular ensemble is induced by a microwave pulse (of duration 1 μs) that sweeps from high to low frequency. Propagation of this microwave pulse is perpendicular to the direction of travel of molecules introduced from the valve. The subsequent relaxation of the molecular ensemble was recorded and digitised by a 100 GS/s oscilloscope (Tektronix DPO72304SX) in the form of a free induction decay (FID) of duration 20μs.

The sequence of polarisation pulse followed by free induction decay is complete within less than 25 μs. Molecules in the expanding jet are spatially-positioned to interact with the microwave pulse for longer than 200 μs. The timescale thus allows for eight iterations of the spectral acquisition per valve pulse. An arbitrary waveform generator, phase-locked dielectric resonant oscillator and oscilloscope are locked to a Rb-clock, which provides a 10 MHz reference that allows coherent averaging of the data in the time domain. The FIDs are co-added in the time domain prior to fast Fourier transformation (FFT) using a Kaiser-Bessel window function to generate the frequency domain spectrum. The resulting spectra have linewidths of

100 kHz (FWHM) consistent with standard deviations of approximately 10 kHz achieved when fitting transitions to the predictions of a model Hamiltonian.

3. Results

3.1 Observed rotational spectra

The rotational spectra of the isotopologues $H_3N \cdots S=C=S$, $H_3N \cdots ^{34}S=C=S$, $H_3N \cdots S=C=^{34}S$, $H_3N \cdots S=^{13}C=S$, $H_3^{15}N \cdots S=C=S$, $H_3^{15}N \cdots ^{34}S=C=S$, $H_3^{15}N \cdots S=C=^{34}S$, $H_3^{15}N \cdots S=^{13}C=S$, $H_3^{15}N \cdots ^{33}S=C=S$ and $H_3^{15}N \cdots S=C=^{33}S$ (absence of a superscript mass number implies the most abundant nuclide) were observed, either in their natural abundance by using an isotopically normal mixture of ammonia and carbon disulphide or a mixture containing an isotopically enriched sample of $^{15}NH_3$. Each spectrum consisted of rotational transitions of the type $J+1 \leftarrow J$, $K \leftarrow K$ expected for the vibrational ground-state of a prolate symmetric-top molecule. Only transitions having $K = 0$ and $K = 1$ had a detectable intensity, presumably because $K = 2$ states lose their room temperature population by transfer to $K = 1$ states during the supersonic expansion of the gas mixture, while transfer of population from $K = 1$ to $K = 0$ states by collision is spin-forbidden. In the ^{14}N-containing species, each $J+1 \leftarrow J$, $K \leftarrow K$ transition exhibited a hyperfine pattern characteristic of coupling of the ^{14}N nuclear spin vector I_N to the framework angular momentum vector J via the interaction of the ^{14}N nuclear electric quadrupole moment with the electric field gradient (efg) at that nucleus. Figure 2 shows a recording of the $J +1 \leftarrow J = 1 \leftarrow 0$, $K \leftarrow K = 0 \leftarrow 0$ transition of the parent isotopologue of $H_3N \cdots S=C=S$ in which the three-component hyperfine structure is resolved. No hyperfine structure was observed in transitions of the ^{15}N-containing molecules, except for those of $H_3^{15}N \cdots ^{33}S=C=S$ and $H_3^{15}N \cdots S=C=^{33}S$, which both carried nuclear quadrupole hyperfine structure characteristic of molecules containing a single ^{33}S nucleus (spin quantum number $I = 3/2$).

The observed frequencies for each isotopologue were accordingly fitted in an iterative nonlinear least squares procedure in which the Hamiltonian given in eqn.(1) was constructed

in the coupled symmetric rotor basis $\boldsymbol{J} + \boldsymbol{I}_{N(or\ S)} = \boldsymbol{F}$ and diagonalized in blocks of the quantum number F by using Western's program PGOPHER.[15]   The form of the Hamiltonian H used was

$$H \;=\; H_R - \frac{1}{6}\mathbf{Q_X}\!:\!\boldsymbol{\nabla}\mathbf{E_X} \qquad (1),$$

in which H_R is the familiar rotational energy operator for a semi-rigid prolate symmetric-top molecule. It was necessary to include only the quartic terms $-D_J J^4$ and $-D_{JK} J^2 J_a^2$ in H_R for a fit commensurate with the estimated error of frequency measurement. In the second term in eq.(1), $\mathbf{Q_X}$ is the electric quadrupole moment dyadic of nucleus X ($= {}^{14}N$ or ${}^{33}S$) and $\boldsymbol{\nabla}\mathbf{E_X}$ is the electric field gradient dyadic at nucleus X.   Since the X nucleus lies on the unique axis a of the prolate symmetric-top molecule, the only independent element of the quadrupole coupling tensor is $\chi_{aa}(X) = eq_{aa}Q_X$ of the X nucleus, where $q_{aa} = \partial^2 V/\partial a^2$, Q_X is the conventional electric quadrupole moment of nucleus X and e is the proton charge.   The spectroscopic constants determined in the final cycle of the least-squares fit for each of the 10 symmetric-top isotopologues are shown in Table 1.
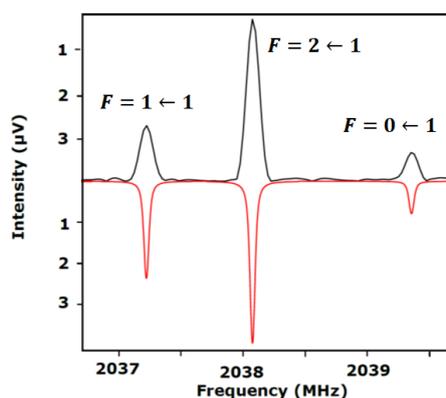
Figure 2.   The $J+1{\leftarrow}J = 1{\leftarrow}0$ transition of the parent isotopologue of $H_3N{\cdots}S{=}C{=}S$ showing the three

${}^{14}N$ nuclear quadrupole hyperfine components. This was recorded by collecting 1.15×10^6 free induction decays.

The red spectrum is that simulated with PGOPHER by using the spectroscopic constants given in Table 1.

Spectroscopic constants determined for the four asymmetric-rotor isotopologues $H_2D^{14}N\cdots^{32}S=^{12}C=^{32}S$, $H_2D^{14}N\cdots^{34}S=^{12}C=^{32}S$, $H_2D^{14}N\cdots^{32}S=^{12}C=^{34}S$, and $HD_2^{14}N\cdots^{32}S=^{12}C=^{32}S$ are included in Table 1. In each case, only $K_{-1} = 0$ transitions could be observed, a familiar consequence of the breaking of C_{3v} symmetry and thereby relaxation of the $K+1\rightarrow K = 1\rightarrow 0$ spin-forbidden propensity rule mentioned earlier. Because the $K_{-1} = 1$ levels are several cm^{-1} higher in wavenumber than the $K_{-1} = 1$ levels in the D species they are susceptible to cooling in the expansion. ^{14}N nuclear quadrupole hyperfine structure was insufficiently resolved for these species and each spectrum was fitted by using the appropriate asymmetric-rotor Hamiltonian to give the only determinable spectroscopic constants $(B+C)/2$ and Δ_J, as included in Table 1. Observed frequencies and the spectroscopic constants determined in the final cycle of the PGOPHER fits for all isotopologues investigated are available in the Supplementary Material.

3.2 *Experimentally determined distance r(N□S)*

The magnitude of the changes in the rotational constants B_0 of the parent species on isotopic substitution at each atom establishes that the order of the atoms is $H_3^{14}N\cdots^{32}S=^{12}C=^{32}S$. The nature of the rotational spectra observed show that the complex is a symmetric-top molecule. The fact that the interaction between the two molecules is very weak (see Section 3.4) suggests that we assume the r_0 geometries of ammonia and carbon disulfide are unchanged on complex formation when determining a r_0 value of the distance $r(N□S)$ in the complex. The r_0 geometry of NH_3 was determined by fitting the ground-state rotational constants[16] B_0 and C_0 of $^{14}NH_3$ and $^{15}NH_3$ isotopologues while that of CS_2 was similarly obtained from a fit of the ground-state rotational constants of several isotopologues measured in a recent high-resolution examination of the Raman spectrum.[17] In each case, Kisiel's program STRFIT[18] was employed and the results are in Table 2. The observed ^{14}N nuclear quadrupole coupling constant of $^{14}NH_3$ is also included in Table 2 for later use.[19]

A fit of $r(N\cdots S)$ to the moments of inertia I_b^0 of the 10 symmetric-top isotopologues with STRFIT by assuming unchanged monomer geometries (as given in Table 2) leads to the very precise value r_0 $(N\cdots S) = 3.3292(1)$ Å.   Inclusion of the D-substituted species gives 3.3288(2) Å for this distance. An r_s version[20] is available through the isotopic substitutions at N and S. The resulting value r_s $(N\cdots S) = 3.311(2)$ Å.   Such analyses do not take into account that the complex is very floppy in the zero-point state, as indicated by a small intermolecular stretching force constant of only ~ 4.0 N m^{-1} (see Section 3.4), which is of similar magnitude to those of inert gas complexes.
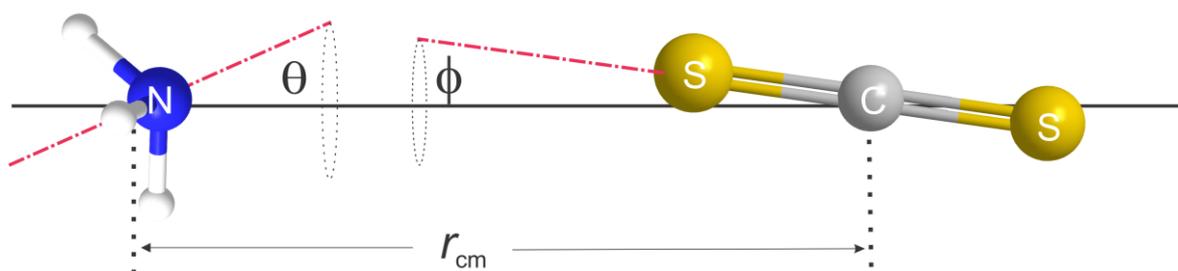
Figure 3.   Definition of r_{cm} and the oscillation angles θ and ϕ used in interpretation of the observed principal moments of inertia I_b^0 of 10 symmetric-top isotopologues of $H_3N\cdots S=C=S$ to give r_{cm} and $r(N\cdots S)$.

It is possible to account for the most serious effects of the zero-point motion of the complex $H_3N\cdots S=C=S$, namely the effects of the intermolecular bending modes, when determining the distance $r(N\cdots S)$ from ground-state moments of inertia. The model of the complex[21] shown schematically in Figure 3 allows for the contribution of these modes, but not the intermolecular stretching mode. Each subunit NH_3 and S=C=S is assumed to execute the indicated angular oscillations, assumed axially symmetric (two-dimensionally isotropic), with respect to its centre of mass, but with the distance r_{cm} between the mass centres fixed (i.e no intermolecular stretching).   In Figure 3, θ is the angle between the line r_{cm} and the C_3 axis of NH_3 and ϕ is the corresponding angle made with the C_∞ axis of CS_2.   By using this model, it

can be shown[21] that I_b^0 of the complex is related to the ground-state principal moments of inertia $I_b^{NH_3}$, $I_c^{NH_3}$ and $I_b^{CS_2}$ of the components (as calculated from their observed rotational constants recorded in Table 2) by

$$I_b^0 \approx \mu r_{cm}^2 + \tfrac{1}{2}I_b^{NH_3}\langle 1 + \cos^2\theta\rangle + \tfrac{1}{2}I_c^{NH_3}\langle \sin^2\theta\rangle + \tfrac{1}{2}I_b^{CS_2}\langle 1 + \cos^2\phi\rangle \qquad (2)$$

In eq.(2), the angular brackets indicate averages taken over the zero-point motion and $\mu = m^{NH_3}m^{CS_2}/(m^{NH_3} + m^{CS_2})$ is the reduced mass for the axially symmetric motion of the subunits.

It is necessary to estimate values of $\theta_{av}= \cos^{-1}\langle\cos^2\theta\rangle^{\frac{1}{2}}$ and $\phi_{av}= \cos^{-1}\langle\cos^2\phi\rangle^{\frac{1}{2}}$ for use in eq.(2). In Section 3.3, it is shown that the angle $\theta_{av} = 27(3)$ ^{o} may be determined from the ^{14}N nuclear quadrupole coupling constant $\chi(^{14}$N), after correction for the change in efg when the CS_2 subunit is brought from infinity to the separation r_{cm}. The change in efg was estimated by calculations for NH_3 and $H_3N\cdots S=C=S$ at the B3LYP/aug-cc-pV6Z level of theory using the Gaussian Electronic Structure program.[22] A detailed analysis of calculations at the B3LYP/aug-cc-pVnZ (n =3, 4, 5 or 6) level for free CS_2 (see Section 3.3) leads to an estimate of $\chi_0(^{33}$S) = -17.1(6) MHz, which when combined in the way discussed in Section 3.3 with the measured values of $\chi(^{33}$S) = -16.495(46) MHz and -16.135(76) MHz for $H_3^{15}N\cdots S=C=^{33}$S and $H_3^{15}N\cdots^{33}S=C=$S, respectively, leads to $\phi_{av}= 10(3)°$. Values of r_{cm} for the ten symmetric-top isotopologues of $H_3N\cdots S=C=S$ investigated here are given in Table 3, which also includes distances $r(N\square S)$ estimated by means of eq.(3).

$$r(N\square S) = r_{cm} - r - r' \qquad (3)$$

where r is the distance of N from the NH_3 mass centre and r' is the distance of the inner S atom from the mass centre of CS_2, as calculated from the r_0 geometries given in Table 2. The mean value of $r(N\square S) = 3.338(10)$ Å is longer than obtained in the simple r_0 fit by 0.009 Å

and represents the best available estimate of this quantity. As expected, it is longer than the equilibrium value $r_e = 3.304$ Å obtained recently[13] from an *ab initio* calculation at the CCSD(T)/aug-cc-pVTZ level. The r_s value 3.311(2) Å is closer to the *ab initio* value but the agreement might be fortuitous.

3.3   Interpretation of the ^{14}N and ^{33}S nuclear quadrupole coupling constants

The determination of the angles θ_{av} and ϕ_{av}, as defined in Section 3.2, relies on interpretations of the observed ^{14}N and ^{33}S nuclear quadrupole coupling constants, respectively. In each case, the observed coupling constant of the complex is first corrected for the additional efg at the nucleus X in question arising from the presence of the other subunit when in the complex. This is assumed to be a small effect and can be calculated as set out below. Then the nuclear quadrupole coupling constant so corrected $\chi_{aa}^{corr}(X)$ is related to its free molecule value $\chi_0(X)$ by the familiar expression

$$\chi_{aa}^{corr}(X) = \frac{1}{2}\chi_0(X)\langle 3\cos^2\tau - 1\rangle \qquad (\tau = \theta \text{ or } \phi) \qquad (4),$$

from which $\langle\cos^2\tau\rangle$ is available. We deal with the case $\tau = \phi$ first.

Unfortunately, a value of $\chi_0(^{33}S)$ for the free CS_2 molecule is unavailable from the usual source, because CS_2 has no pure rotational spectrum. Measurements of nmr spectra of liquid CS_2 have yielded the values -13.8 MHz[23] and -14.9(3) MHz[24] and an early *ab initio* calculated value is available.[25] Here we employ the following approach. Density functional calculations carried out at the B3LYP/aug-cc-pVnZ level of theory ($n = 3, 4, 5$ and 6) with the Gaussian electronic structure package[22] were used to evaluate the ^{33}S nuclear quadrupole coupling constant $\chi_0(^{33}S)$ for each of the three molecules CS, OCS and CS_2. For each n, the basis function aug-cc-pV(n +d)Z was used for S, because S requires a tight d-function. The results for the different basis sets are recorded in Table 4. The zero-point values of this coupling

constant are known to high accuracy for CS[26] and OCS[27] and are included in Table 4. It is noted from Table 4 that from $n = 5$ to $n = 6$ the calculated coupling constants change by 0.03 MHz, 0.11 MHz and 0.17 MHz, for CS, CS_2 and OCS, respectively. Column 5 of Table 4 gives the ratios $\chi_{obs.}(^{33}S)/\chi_{calc.}(^{33}S)$ for CS and OCS, while columns 6 and 7 give the values predicted for $\chi_{obs.}(^{33}S)$ of CS_2 by assuming that the ratios that apply for CS and OCS, respectively, also apply to CS_2. Since there is no reason to prefer the results in either column 6 or 7, it seems reasonable to use the mean of the two B3LYP/aug-cc-pV6Z values, that is to assume $\chi_0(^{33}S)$ = -17.1(6) MHz as the best estimate for the CS_2 free molecule coupling constant.

Correction of the observed ^{33}S nuclear quadrupole coupling constant of the isotopologues $H_3{}^{15}N\cdots^{33}S=C=S$ and $H_3{}^{15}N\cdots S=C=^{33}S$ for the effects of the efg at the appropriate S due to the presence of the NH_3 subunit can be made readily from the observations collected in Table 5. This table lists the two (inner and outer) ^{33}S coupling constants for the isotopologue $H_3N\cdots^{33}S=C=^{33}S$ when calculated at the B3LYP/aug-cc-pVnZ ($n = 3$-6) levels of theory. Also given in Table 5 is the mean of these two coupling constants (column 4) and the corresponding values of the calculated coupling constant for the free molecule $^{33}S=C=S$ in column 5. We note that the difference between columns 4 and 5 is negligible in the present context, that is the mean of the inner and outer ^{33}S coupling constants of $H_3N\cdots^{33}S=C=^{33}S$ is essentially identical to the ^{33}S coupling constant of the free CS_2 molecule. Since the calculations refer to the C_{3v} equilibrium geometry of $H_3N\cdots^{33}S=C=^{33}S$, in which there is no zero-point oscillation of the subunits ($\theta = \phi = 0$), this analysis suggests that the mean of the values of the $\chi_{obs.}(^{33}S)$ for $H_3{}^{15}N\cdots^{33}S=C=S$ and $H_3{}^{15}N\cdots S=C=^{33}S$ should be used as $\chi_{aa}^{corr}(^{33}S)$ (*i.e.* corrected for the efg due to NH_3) when deriving $\langle\cos^2\phi\rangle$ from eq.(4). Thus, $\chi_{aa}^{corr}(^{33}S)$ = (-16.14 -16.50)/2 = -16.32 MHz. When $\chi_{aa}^{corr}(^{33}S)$ = -16.32 MHz and $\chi_0(^{33}S)$ = -17.1(6) MHz are used in eq.(4), the result is $\phi_{av} = \cos^{-1}\langle\cos^2\phi\rangle^{\frac{1}{2}} = 10(3)$ °.

Comparison of $\chi_0(^{14}N)$ for the free ammonia molecule with that of $H_3N\cdots S=C=S$ when both are calculated at the B3LYP/aug-cc-pVnZ level of theory shows a constant difference of only ~ 0.04 MHz for n in the range 3 to 6. For example, the two values calculated

at the $n = 6$ level are -4.438 MHz for NH_3 and -4.401 MHz for $H_3N\cdots S=C=S$. Thus, the free

molecule value[19] $\chi_0(^{14}N)$ = -4.090 MHz (included in Table 2) can be corrected to

$\chi_0^{corr}(^{14}N)$ = -4.090 - 0.04 MHz = -4.13 MHz, which when used in eq.(4) with the observed

value $\chi(^{14}N)$ = -2.846(4) MHz for $H_3^{14}N\cdots SCS$ gives $\theta_{av}= \cos^{-1}\langle\cos^2\theta\rangle^{\frac{1}{2}} = 27°$, with a liberal

range of $\pm 3°$ assumed from consideration of the related average $\langle\theta^2\rangle^{1/2}$ determined in Section

3.4.

3.4   Intermolecular stretching and bending force constants

There are two measures of the strength of the interaction of NH_3 and S=C=S to form

the complex $H_3N\cdots S=C=S$. The first is the dissociation energy D_e. The second is the

intermolecular stretching force constant k_σ, which is a measure of the resistance to an

infinitesimal displacement along the weak bond direction.   Millen[29] showed that k_σ is simply

related to the centrifugal distortion constant D_J and the rotational constant B_0 for symmetric-

top complexes such as $H_3N\square S=C=S$ by

$$k_\sigma = \left(16\pi^2\mu B_0^3/D_J\right)\{1 - (B_0/B^{NH_3}) - (B_0/B^{CS_2})\} \qquad (5),$$

where μ is as defined earlier and B^{NH_3} and B^{CS_2} are rotational constants of the separate

components.   The derivation of eqn. (5) assumes rigid subunits and ignores terms beyond

quadratic in the potential energy function.   The values of k_σ for the symmetric-top

isotopologues calculated with the aid of eqn. (5) by using the ground-state spectroscopic

constants of the complex (Table 1) and the separate components (Table 2) are included in Table

3. The mean is 3.97(5) N m^{-1}, if the outlying final entry is ignored, and is slightly smaller than

that (k_σ = 5.3 N m^{-1}) recently calculated[13] at the CCSD(T)/aug-cc-pVTZ level of theory. The

difference arises in part because, strictly, equilibrium rather than zero-point spectroscopic

constants should be used in eq.(5).

The intermolecular bending force constant $k_{\theta\theta}$ can also be estimated from centrifugal distortion constants. If the model for the motion of the subunits discussed in Section 3.2 and illustrated in Figure 3 is assumed and each subunit is again described as a two-dimensional isotropic harmonic oscillator, the quadratic force constant $k_{\theta\theta}$ is related to the centrifugal distortion constant $D = 2D_J + D_{JK}$ by[29]

$$k_{\theta\theta} = (2h/D)B_0^2[B_0/B^{\mathrm{NH_3}} - 1]^2 \qquad (6)$$

Eqn. (6) applies to symmetric-top isotopomers of $H_3N\square S=C=S$ only. Values of $k_{\theta\theta}$ estimated by using $D = 2D_J + D_{JK}$ and B_0 from Table 1 and $B^{\mathrm{NH_3}}$ for the free ammonia molecule (Table 2) are included in Table 3 for the symmetric-top isotopologues of the complex. The errors transmitted from those in the centrifugal distortion constants when using eq.(6) are small and presumably differences in $k_{\theta\theta}$ outside the quoted errors arise mainly from limitations of the model used to obtain eq.(6).

An alternative to the angle $\theta_{\mathrm{av}} = \cos^{-1}\langle\cos^2\theta\rangle^{\frac{1}{2}}$ defined in Section 3.2 is $\langle\theta^2\rangle^{1/2}$, which can be estimated from $k_{\theta\theta}$. It has been shown that $\langle\theta^2\rangle$ is related to $k_{\theta\theta}$ by means of the expression[30]

$$\langle\theta^2\rangle = (h/2\pi)\left(k_{\theta\theta}I_b^{\mathrm{NH_3}}\right)^{-1/2} \qquad (7)$$

if the motion of the NH_3 subunit in the symmetric-top complex can be treated as a two-dimensional isotropic oscillator. Using the values of $I_b^{\mathrm{NH_3}}$ implied by the monomer rotational constants given in Table 2, we estimate that the mean value $\langle\theta^2\rangle^{1/2} = 31.0(1)$ ° for the ten symmetric-top isotopologues of $H_3N\square S=C=S$. If $\langle\theta^2\rangle^{1/2}$ is not too large, we can assume that $\langle\theta^2\rangle^{1/2} \approx \cos^{-1}\langle\cos^2\theta\rangle^{1/2}$, which is consistent with the choice of the range for the angle $\theta_{\mathrm{av}} = 27(3)$ ° used in connection with the geometry determination discussed in Section 3.2.

4. Discussion

The ground-state rotational spectra of 14 isotopologues of the complex $H_3N\square S=C=S$ formed between ammonia and carbon disulphide in the gas phase have been analysed to yield rotational constants, centrifugal distortion constants and, where appropriate, ^{14}N and ^{33}S nuclear quadrupole coupling constants. The nature of the spectra and the changes that accompany the isotopic substitutions establish that the complex is a symmetric-top molecule of C_{3v} symmetry with the atoms in the order $H_3N\square S=C=S$. Thus, the intermolecular bond is between the non-bonding electron pair on N and the electrophilic region near S on the C_3 axis of the complex, that is it is the type of non-covalent interaction now referred to as a chalcogen bond. A simple model used to account for the contribution of the angular oscillations to the zero-point motion leads to the distance $r(N\cdots S) = 3.338(10)$ Å, which is, as expected, longer than the equilibrium value 3.304 Å obtained from a recent *ab initio* calculation [13] at the CCSD(T)/aug-cc-pVTZ level. Interpretations of the centrifugal distortion constants of the complex lead to the intermolecular stretching and bending force constants $k_\sigma = 3.97(2)$ N m^{-1} and $k_{\theta\theta} = 4.63(3) \times 10^{-21}$ J, which indicate that intermolecular chalcogen bond is weak. For comparison, values of $k_\sigma = 12.2$ and 12.7 N m^{-1} and $k_{\theta\theta} = 27.5 \times 10^{-21}$ and 42.2×10^{-21} J have been reported by these methods[29] for the hydrogen-bonded complex $H_3N\cdots HCN$ and the halogen-bonded complex $H_3N\cdots Cl_2$, respectively. The value of $\langle\theta^2\rangle^{1/2} = 31°$ determined from $k_{\theta\theta}$ has been shown to be consistent with the angular oscillation $\theta_{av} = \cos^{-1}\langle\cos^2\theta\rangle^{\frac{1}{2}}$ $= 27(3)°$ of the NH_3 subunit deduced from the ^{14}N nuclear quadrupole coupling constant.

Supplementary Material

Outputs from the final cycle of the PGOPHER fits of transitions of each isotopologue investigated are available as Supplementary Material.

References

1.   A.C. Legon, Angew. Chem. Int. Ed. Engl., **38**, 2686-2714 (1999).

2.   P. Metrangolo, H. Neukirch, T. Pilati and G. Resnati, *Acc. Chem. Res.*, **38**, 386-395, 2005.

3.   E. Arunan, G. R. Desiraju, R. A. Klein, J. Sadlej, S. Scheiner, I. Alkorta, D. C. Clary, R. H. Crabtree, J. J. Dannenberg, P. Hobza, H. G. Kjaergaard, A. C. Legon, B. Mennucci, and D. J. Nesbitt, *Pure and Applied Chemistry*, **83**, 1637-1641 (2011).

4.   G. R. Desiraju, P. S. Ho, L. Kloo, A. C. Legon, R. Marquardt, P. Metrangolo, P. A. Politzer, G. Resnati and K. Rissanen, *Pure and Applied Chemistry*, **85**, 1711-1713 (2013).

5.   W. Wang,W., B. Ji and Y. Zhang, *J. Phys. Chem. A*, **113**, 8132–8135 (2009)

6.   S. Zahn, R. Frank, E. Hey-Hawkins and B. Kirchner, *Chem. Eur., J.*, **17**, 6034–6038 (2011).

7.   A.Bauzá, T. J. Mooibroek and A. Frontera, *Angew. Chem. Int. Ed.*, **52**, 12317–12321, 2013.

8.   A. C. Legon and N. R. Walker, *Phys. Chem. Chem. Phys*., **20**, 19332-19338 (2018).

9.   A. C. Legon, *Phys. Chem. Chem. Phys*., **19**, 14884-14896   (2017).

10.   G. T. Fraser, K. R. Leopold and W. Klemperer, *J. Chem. Phys.,* **81**, 2577-2584, (1984).

11.   B. J. Deppmeier, A. J. Driessen, T. S. Hehre, W. J. Hehre, J. A. Johnson, P. E. Klunzinger, J. M. Leonard, I. N. Pham, W. J. Pietro, J. Yu, Y. Shao, L. Fusti-Molnar, Y. Jung,J. Kussmann, C. Ochsenfeld, S. T. Brown, A. T. B. Gilbert,L. V. Slipchenko,S. V. Levchenko, D. P. O'Neill, R. A. Di Stasio Jr., R. C. Lochan, T. Wang, G. J. O. Beran, N. A. Besley, J. M. Herbert, C. Y. Lin, T. Van Voorhis, S. H. Chien, A. Sodt, R. P. Steele, V. A. Rassolov, P. E. Maslen, P. P. Korambath,R. D. Adamson, B. Austin, J. Baker, E. F. C. Byrd, H. Dachsel,R. J. Doerksen, A. Dreuw, B. D. Dunietz, A. D. Dutoi,T. R. Furlani, S. R. Gwaltney, A. Heyden, S. Hirata, C.-P.Hsu, G. Kedziora, R. Z. Khalliulin, P. Klunzinger, A. M. Lee, M. S. Lee, W. Liang, I. Lotan, N. Nair, B. Peters, E. I. Proynov, P. A. Pieniazek, Y. M. Rhee, J. Ritchie, E. Rosta, C. D. Sherrill, A. C. Simmonett, J. E. Subotnik, H. L. Woodcock III, W. Zhang, A. T. Bell, A. K. Chakraborty, D. M. Chipman, F. J. Keil, A. Warshel, W. J. Hehre, H. F. Schaefer III, J. Kong, A. I. Krylov, P. M. W. Gill and M. Head-Gordon, SPARTAN'14 Mechanics Program: (Win/64b) Release 1.1.8, Wavefunction Inc., SPARTAN Inc., 2014.

12.   T. Ogata and F. J. Lovas, *J. Mol. Spectrosc*., **162**, 505-512, (1992).

13.   I Alkorta and A. C. Legon, *Molecules,* **23**, 2250-2265 (2018).

14.   D.P. Zaleski, S.L. Stephens, N.R. Walker, *Phys. Chem. Chem. Phys*. **16**, 25221–25228 (2014).

15.   PGOPHER, a Program for Simulating Rotational Structure, Designed by C.M. Western, University of Bristol, version 6.0.202, 2010. Available at: <http:// pgopher.chm.bris.ac.uk>.

16.   P. Helminger, F. De Lucia and W. Gordy, *J. Mol. Spectrosc*., **39**, 94-97,(1971).

17.   C. Schrötera, J. C. Lee and T. Schultza, *Proc. Nat. Acad. Sci*., **115**, 5072–5076 (2018).

18.   Z. Kisiel, *J. Mol. Spectrosc.*, **218**, 58-67 (2003).

19.   M. D. Marshall and J. S. Muenter, *J. Mol. Spectrosc.*, **85**, 322-326 (1981).

20.   C. C. Costain, *J. Chem. Phys.*, **29**, 864-874, (1958).

21.   G. T. Fraser, K. R. Leopold, D. D. Nelson Jr., A Tung and W. Klemperer, *J. Chem. Phys.*, **80**, 3073-3077 (1984).

22.   M. J. Frisch, G. W. Trucks, H. B. Schlegel, G. E. Scuseria, M. A. Robb, J. R. Cheeseman, G. Scalmani, V. Barone, B. Mennucci, G. A. Petersson, H. Nakatsuji, M. Caricato, X. Li, H. P. Hratchian, A. F. Izmaylov, J. Bloino, G. Zheng, J. L. Sonnenberg, M. Hada, M. Ehara, K. Toyota, R. Fukuda, J. Hasegawa, M. Ishida, T. Nakajima, Y. Honda, O. Kitao, H. Nakai, T. Vreven, J. A. Montgomery, Jr., J. E. Peralta, F. Ogliaro, M. Bearpark, J. J. Heyd, E. Brothers, K. N. Kudin, V. N. Staroverov, T. Keith, R. Kobayashi, J. Normand, K. Raghavachari, A. Rendell, J. C. Burant, S. S. Iyengar, J. Tomasi, M. Cossi, N. Rega, J. M. Millam, M. Klene, J. E. Knox, J. B. Cross, V. Bakken, C. Adamo, J. Jaramillo, R. Gomperts, R. E. Stratmann, O. Yazyev, A. J. Austin, R. Cammi, C. Pomelli, J. W. Ochterski, R. L. Martin, K. Morokuma, V. G. Zakrzewski, G. A. Voth, P. Salvador, J. J. Dannenberg, S. Dapprich, A. D. Daniels, O. Farkas, J. B. Foresman, J. V. Ortiz, J. Cioslowski, and D. J. Fox, *Gaussian 09, Revision D.01*, Gaussian, Inc., Wallingford CT, 2013.

23.   R. R. Vold, S.W. Sparks and R. L. Vold, *J. Magn. Res.*, **30**, 497-503 (1978).

24.   A. Loewenstein and D. Igner, *J. Phys. Chem.*, **92**, 3124-2129 (1988).

25.   M. H. Palmer, *Z. Naturforsch.*, **47a**, 203-216 (1992).

26.   E. Kim and S. Yamamoto, *J. Mol. Spectrosc.*, **219**, 296-304 (2003).

27.   J. M. L. J. Reinartz and A. Dymanus, *Chem. Phys. Lett.*, **24**, 346-349 (1974).

28.   D. J. Millen, *Can. J. Chem.*, **63**, 1477-1479 (1985).

29.   A.C. Legon and D.G. Lister, *Chem. Phys. Lett.*, **238,** 156-162 (1995). Note that the version of eqn. (6) given in this reference has the factor of 2 in the denominator instead of the numerator.

30. P. Cope, D.J. Millen and A.C. Legon, *J. Chem. Soc. Faraday Trans. 2*, **83**, 2163-2170 (1987).

Tables

Table 1 Experimentally determined spectroscopic constants for all observed isotopologues of H$_3$N···S=C=S

Isotopologue	B_0 /MHz	D_J /kHz	D_{JK} /MHz	$\chi(^{14}N)$ /MHz	$\chi(^{33}S)$ /MHz	N^b	σ_{RMS}^{c} /kHz
H$_3$N···S=C=S	1018.96800(25)[a]	0.6688(25)	0.29576(20)	-2.8459(37)	-	55	7.5
H$_3$N···^{34}S=C=S	1017.25911(24)	0.6603(20)	0.29477(21)	-2.8487(55)	-	29	5.5
H$_3$N···S=^{13}C=S	1017.34286(49)	0.6683(37)	0.29475(38)	-2.801(27)	-	18	8.6
H$_3$N···S=C=^{34}S	995.27480(35)	0.6319(28)	0.28326(30)	-2.8493(88)	-	27	7.6
H$_3$^{15}N···S=C=S	988.08909(33)	0.6390(27)	0.27551(25)	-	-	17	5.8
H$_3$^{15}N···^{34}S=C=S	986.68068(39)	0.6331(36)	0.27482(32)	-	-	16	6.8
H$_3$^{15}N···S=^{13}C=S	986.40821(55)	0.6556(44)	0.26827(31)	-	-	8	4.7
H$_3$^{15}N···S=C=^{34}S	965.04052(57)	0.6082(54)	0.26541(25)	-	-	14	7.9
H$_3$^{15}N···^{33}S=C=S	987.37738(68)	**{0.6331(36)}[d]**	0.27694(50)	-	-16.135(76)	18	14.2
H$_3$^{15}N···S=C=^{33}S	976.28988(68)	**{0.6082(54)}[d]**	0.26637(97)	-	-16.495(29)	22	14.1
H$_2$DN···S=C=S	981.5589(12)[e]	0.646(10)	-	-	-	6	14.1
HD$_2$N···S=C=S	947.4938(13)	0.613(11)	-	-	-	6	14.9
H$_2$DN···^{34}S=C=S	980.8068(19)	0.611(16)	-	-	-	5	19.1
H$_2$DN···S=C=^{34}S	958.7355(12)	0.604(10)	-	-	-	6	14.4

[a] Numbers in parentheses are one standard deviation in units of the last significant figure.

[b] Number of structural components of the fit.

[c] Root mean square deviation of the fit.

[d] Value for D_J fixed at that for H$_3$^{15}N···^{34}S=C=S and H$_3$^{15}N···S=C=^{34}S isotopologue, respectively. Only three J available for H$_3$^{15}N···^{33}S=C=S and H$_3$^{15}N···S=C=^{33}S, and three J dependent terms cannot be well defined.

[e] $(B + C)/2$ for asymmetric-top isotopologues containing D

Table 2. Some molecular properties of ammonia and carbon disulphide

Molecule	B_0/MHz	C_0/MHz	r_0 geometry	$\chi_0(^{14}N)$/MHz	$\chi_0(^{33}S)$/MHz
$^{14}NH_3$	298115.37[a]	187405[b]	r_0(N–H) =1.01557 Å[c] ∠(HNH) =107.277°	-4.08983(2)[d]	–
$^{15}NH_3$	297388.12[a]	187405[b]	–	–	
$^{32}S{=}^{12}C{=}^{32}S$	3271.5170(7)[e]	3271.5170(7)[e]	r_0(C=S) =1.55427(1)[f] Å	–	-17.1(6)[g]

[a]Ref.16. [b]Calculated from the r_0 geometry. [c]Calculated by fitting B_0 values of $^{14}NH_3$ and $^{15}NH_3$. [d]Ref.19.
[e]Ref.17. [f]Calculated by fitting B_0 values of six isotopologues of S=C=S given in ref.17. [g]Calculated *ab initio*,
See Section 3.3 for details.

Table 3.   Some properties of the complex $H_3N \cdots S=C=S$ derived from the rotational spectra of ten symmetric-top isotopologues

Isotopologue	$r_{cm}/Å$ [a]	$r(N \cdots S)/Å$ [a]	$k_\sigma/(N\ m^{-1})$ [b]	$10^{21}\ k_{\theta\theta}/J$ [c]
$H_3N \cdots S=C=S$	4.959(10)	3.338(10)	3.95(2)	4.600(3)
$H_3N \cdots S=C={}^{34}S$	4.999(10)	3.338(10)	3.91(2)	4.583(5)
$H_3N \cdots S={}^{13}C=S$	4.959(10)	3.338(10)	3.95(2)	4.600(6)
$H_3N \cdots {}^{34}S=C=S$	4.920(10)	3.339(10)	3.95(1)	4.600(14)
$H_3{}^{15}N \cdots S=C=S$	4.954(10)	3.337(10)	4.01(2)	4.643(5)
$H_3{}^{15}N \cdots S=C={}^{34}S$	4.994(10)	3.337(10)	3.93(3)	4.599(4)
$H_3{}^{15}N \cdots S={}^{13}C=S$	4.954(10)	3.337(10)	3.89(3)	4.751(5)
$H_3{}^{15}N \cdots {}^{34}S=C=S$	4.915 (10)	3.338(10)	4.00(2)	4.642(7)
$H_3{}^{15}N \cdots {}^{33}S=C=S$	4.934(10)	3.338(10)	…	4.613(8)
$H_3{}^{15}N \cdots S=C={}^{33}S$	4.974(10)	3.337(10)	…	4.689(18)

[a]Calculated by using eq.(2).   [b]Calculated by using eq.(5)   [c]Calculated by using eq.(6)

Table 4. Calculated values of the ^{33}S nuclear quadrupole coupling constant of CS_2, CS and OCS at the B3LYP/aug-cc-pV(n + d)Z level of theory for n = 3,4,5 and 6 and its estimated value for the zero-point state of CS_2

Molecule	Basis function aug-cc-pVnZ for B3LYP calculation	$\chi_{calc.}(^{33}S)$ /MHz	$\chi_{obs.}(^{33}S)$ /MHz	$\chi_{obs.}(^{33}S)$ /$\chi_{calc.}(^{33}S)$	Est. value $\chi_{obs.}(^{33}S)$/ MHz for CS_2 from CS ratio in col.5	Est. value $\chi_{obs.}(^{33}S)$/ MHz for CS_2 from OCS ratio in col. 5
CS_2	n = 6	-16.845	….	….	-17.750	-16.520
	n = 5	-16.958	….	….	-17.819	-16.534
	n = 4	-14.934	….	….	-16.471	-16.299
	n = 3	-14.966	….	….	-15.442	-16.162
CS	n = 6	+12.172	+12.8256(2)[a]	1.0537		
	n = 5	+12.206		1.0508		
	n = 4	+11.629		1.1029		
	n = 3	+12.430		1.0318		
OCS	n = 6	-29.692	-29.118(1)[b]	0.9807		
	n = 5	-29.865		0.9750		
	n = 4	-26.679		1.0914		
	n = 3	-26.964		1.0799		

[a] Ref.26. [b] Ref.27.

Table 5. ^{33}S nuclear quadrupole coupling constants of $H_3N \cdots ^{33}S=C=^{33}S$ and $^{33}S=C=S$ calculated at the B3LYP/aug-cc-pV(n+d)Z level of theory.

Basis	$H_3N \cdots ^{33}S_i=C=^{33}S_o$			$^{33}S=C=S$ $\chi(^{33}S_{CS_2})/$ MHz	Difference $\{\chi(^{33}S_{av}) - \chi(^{33}S_{CS_2})\}$ /MHz
	$\chi(^{33}S_i)$/MHz[a]	$\chi(^{33}S_o)$/MHz[b]	$\chi(^{33}S_{av})$/MHz[c]		
$n = 3$	-14.167	-15.540	-14.854	-14.966	0.075 0.112
$n = 4$	-14.198	-15.539	-14.869	-14.934	0.045 0.065
$n = 5$	-16.230	-17.646	-16.938	-16.958	0.020
$n = 6$	-16.055	-17.494	-16.775	-16.845	0.070

[a]Subscript i = inner.   [b]Subscript o =outer.   [c]Subscript av indicates the average of i and o values.